CrossMark
click for updates

Freeze-dried multiscale porous nanofibrous three dimensional scaffolds for bone regenerations

Maryam Sadat Khoramgah[1], Javad Ranjbari[1], Hojjat-Allah Abbaszadeh[2,3], Fatemeh Sadat Tabatabaei Mirakabad[1], Shadie Hatami[4,5], Simzar Hosseinzadeh[6,7*], Hossein Ghanbarian[8,9*]

[1] Department of Medical Biotechnology, School of Advanced Technologies in Medicine, Shahid Beheshti University of Medical Sciences, Tehran, Iran

[2] Laser Application in Medical Sciences Research Center, Shahid Beheshti University of Medical Sciences, Tehran, Iran

[3] Hearing Disorders Research Center, Shahid Beheshti University of Medical Sciences, Tehran, Iran

[4] Institute of NanoEngineering and MicroSystems National Tsing Hua University Hsinchu 30013, Taiwan

[5] Department of Power Mechanical Engineering National Tsing Hua University Hsinchu 30013, Taiwan

[6] Medical Nanotechnology and Tissue engineering Research Center, Shahid Beheshti University of Medical Sciences, Tehran, Iran

[7] Department of Tissue Engineering and Applied Cell Sciences, School of Advanced Technologies in Medicine, Shahid Beheshti University of Medical Sciences, Tehran, Iran

[8] Cellular and Molecular Biology Research Center, Shahid Beheshti University of Medical Sciences, Tehran, Iran

[9] Urogenital Stem Cell Research Center, Shahid Beheshti University of Medical Sciences, Tehran, Iran

Article Info

Abstract

Introduction: Simulating hydrophobic-hydrophilic composite face with hierarchical porous and fibrous architectures of bone extracellular matrix (ECM) is a key aspect in bone tissue engineering. This study focused on the fabrication of new three-dimensional (3D) scaffolds containing polytetrafluoroethylene (PTFE), and polyvinyl alcohol (PVA), with and without graphene oxide (GO) nanoparticles using the chemical cross-linking and freeze-drying methods for bone tissue application. The effects of GO on physicochemical features and osteoinduction properties of the scaffolds were evaluated through an in vitro study.

Methods: After synthesizing the GO nanoparticles, two types of 3D scaffolds, PTFE/PVA (PP) and PTFE/PVA/GO (PPG), were developed by cross-linking and freeze-drying methods. The physicochemical features of scaffolds were assessed and the interaction of the 3D scaffold types with human adipose mesenchymal stem cells (hADSCs) including attachment, proliferation, and differentiation to osteogenic like cells were investigated.

Results: GO nanoparticles were successfully synthesized with no agglomeration. The blending of PTFE as a hydrophobic polymer with PVA polymer and GO nanoparticles (hydrophilic compartments) were successful. Two types of 3D scaffolds had nano topographical structures, good porosities, hydrophilic surfaces, thermal stabilities, good stiffness, as well as supporting the cell attachments, proliferation, and osteogenic differentiation. Notably, GO incorporating scaffolds provided a better milieu for cell behaviors.

Conclusion: Novel multiscale porous nanofibrous 3D scaffolds made from PTFE/ PVA polymers with and without GO nanoparticles could be an ideal candidate for bone tissue engineering as a 3D template.
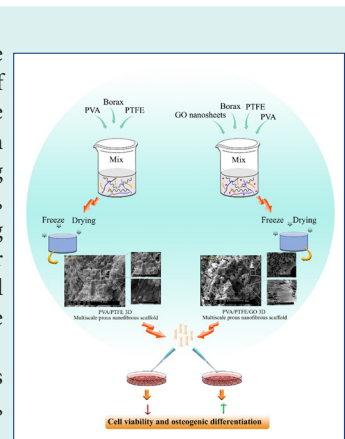
Introduction

The demand for bone substitutes has been increasing globally.[1,2] Tissue engineers focus more on the fabrication of different types of bone substitutes with or without stem cells/progenitor cells and growth factors for repairing bone defects.[3,4] Simulating the natural bone extracellular matrix (ECM) with hydrophobic-hydrophilic composite faces of heterogeneous materials and hierarchical porous and fibrous architectures as 3D scaffolds that provide surfaces for cell attachment, proliferation, migration,

*Corresponding authors: Simzar Hosseinzadeh, Email: S.hosseinzadeh@sbmu.ac.ir, atsa364@gmail.com; Hossein Ghanbarian, Email: hghanbarian@sbmu.ac.ir

differentiation, mineralization, neovascularization, and finally the formation of new tissue is a most important aspect in bone tissue engineering (BTE).[3,5] The key fibrous proteins of bone ECM, collagen and elastin, have hydrophobic/hydrophilic faces due to the complicated arrangement of their hydrophilic and hydrophobic amino acids and domains. They play important roles in osteoblasts differentiation,[6] mineralization process,[7-9] mechanical properties,[10,11] and also bone hierarchical structure.[7]

To date, a vast range of hydrophilic, hydrophobic, and also amphiphilic natural or synthetic materials have been fabricated and used in mimicking bone ECM architecture. However, their constraints make new approaches, and materials mixture with or without cells is necessary to improve the performance of their counterparts.[2,6,12]

Recently, utilization of hydrophobic materials and hydrophobic/hydrophilic interactions in tissue scaffolds such as hydrophobic association hydrogels has become an exciting research topic in the rapidly developing field of tissue engineering due to their critical roles in the biological system, especially in mechanical performance.[13,14] It was demonstrated that surface and matrix hydrophobicity has a critical effect in protein adsorption,[15] osteoblast attachment,[16] biomineralization process,[17] and promoting the healing of bone defects.[18]

Polytetrafluoroethylene (PTFE), the most attractive hydrophobic synthetic polymer, is a physiologically inert molecule with helical linear chains of carbon and fluorine and has been widely used in biomedical fields such as arterial grafts, medical ports, hernia surgical mesh, as well as suture and reconstructive facial surgery.[19] PTFE has desirable mechanical and thermochemical stability and is a replacement for metal and other materials in medicine. However, like most of polymers, PTFE has poor cell-adhesiveness properties.[19] Chemical and physical modifications such as peptide immobilization,[20] plasma modification,[21] and photochemical methods[22] were used to improve the cell adhesive properties of PTFE. These strategies are hampered by the fact that inside the 3D porous structure as tissue scaffolds are not readily treatable.

The development of new and advanced multicomponent systems in the form of composite or nanocomposite materials have been utilized to improve material properties for tissue engineering application.[23] Recently, a study reported the electrospun nanofiber membranes to be formed from PTFE-PVA-boric acid-H2O gel-spinning solutions successfully.[24]

Polyvinyl alcohol (PVA) has been widely used as a hydrogel scaffold alone or in combination with different polymers and nanoparticles for tissue engineering applications. PVA has outstanding bio-physicochemical properties such as good chemical resistance, thermal stability, processability, good film-forming, capacity high crystal modulus, high hydrophilicity, biocompatibility, complete biodegradability, and nontoxicity. The major functional groups of PVA is hydroxyl groups that ease its blending capacity to other polymers as well as cell adhesion.[25,26] Many studies have been conducted on blending PVA with other materials such as graphene oxide nanoparticles[27] to prepare bio-physicochemical stronger hydrogel. Incorporation of carbon-based nanoparticles into various polymer matrices opened up a remarkable research area in the composite material fields.[28] Graphene oxide (GO) nanoparticles, two-dimensional sheet consisted of hydrophobic π domains and oxygen functional groups such as –OH, –COOH and –O– groups have absorbed great attention in recent years. GO nanoparticles could be readily dispersed within water or another hydrophilic polymer due to the oxygen functional groups and enhancing the physical, chemical, mechanical, and thermal properties of other materials. Furthermore, GO nanoparticles have excellent biocompatibility, protein absorption, and support cellular attachment proliferation and differentiation, as well as good apatite-forming ability which makes it a desirable polymer in the field of BTE.[29,30]

In the present work, we reported a novel freeze-dried high porous nanofibrous 3D scaffold formed from PTFE, PVA, and GO nanoparticles and explored structural, thermal, and mechanical features, as well as attachment and differentiation of human adipose mesenchymal cells (hADSCs) to bone-like cells on the scaffolds in an in vitro study.

Materials and Methods
Materials
All chemical reagents including sulfuric acid 98%, NaNO3, KMnO4, H2O2 30% v/v, boric acid, glutaraldehyde, paraformaldehyde, 4′, 6-diamidino-2-phenylindole stain (DAPI), 3-[4, 5-dimethylthiazol-2-yl]-2, 5-diphenyl tetrazolium bromide (MTT reagent), dimethyl sulfoxide (DMSO), triton X-100, Alizarin Red S (ARS) dye, Graphite powder 20 μm synthetic, and PVA powder with 85 000-124 000 molecular weight and 99+% hydrolyzed were purchased from Sigma-Aldrich, Germany. For in vitro cell study, reagents including phosphate-buffered saline (PBS), collagenase type I, DMEM/F-12 (Dulbecco's Modified Eagle Medium/Nutrient Mixture F-12F), fetal bovine serum (FBS), antibiotics (penicillin, streptomycin), and trypsin/ethylenediaminetetraacetic were purchased from Gibco, Germany. The osteogenic differentiation medium containing DMEM-F12, 10% FBS, 2 mM L-glutamine, 100 U/mL penicillin, 100 μg/mL streptomycin, 20 mM β-glycerol phosphate, 100 nM dexamethasone, 50 μM ascorbic acid was purchased from Bioidea, Iran.

Synthesis and characterization of GO nanoparticles
Modified hummers method[31] was adopted to prepare GO nanoparticles. In brief, a mixture of 0.5 g graphite powder and 23 mL sulfuric acid 98% were prepared and 0.5 g NaNO3 and 3 g KMnO4 were added into the mixture

gradually. After about 10 minutes, the solution was stirred for 3 hours at 35°C. Then, 40 mL deionized water and 3 mL H2O2 30% v/v were added to the solution, respectively. The solution was filtered and washed repeatedly to remove the impurities. Finally, the exfoliate GO nanosheets were obtained by sonication (100 kHz, 120 W, 40 minutes) and centrifugation (3500 rpm, 30 minutes). The prepared nanoparticles were characterized by transmission electron microscopy (TEM; JEOL Inc., EM2100).

Fabrication of 3D nanocomposite scaffolds

PVA solution (16% w.t) was prepared by solving PVA powder (Mw 85,000-124,000, 99+% hydrolyzed) in deionized water by continuous stirring at 80°C for about 2 hours. Blended solutions of PVA and PTFE (CAS Number 9002-84-0) were prepared by mixing them at ratios of 22: 78 (PVA: PTFE) with thoroughly stirring for 1 hour to obtain a homogenous mixture. Afterward, 0.005 g of GO nanoparticles was added to the blended solutions of PVA and PTFE and sonicated for 30 minutes (only PPG scaffolds). Then 1 μL/mL boric acid at a concentration of 4% was added to the blended solution of PVA/PTFE/GO nanoparticles as a crosslinking agent and freeze-dried (Christ GAMMA 1-16 LSC Freeze Dryers) for 18 hours at -40°C to obtain PVA/PTFE (PP) and PVA/PTFE/GO (PPG) 3D scaffolds. Prepared 3D scaffolds were cylinder-shaped with 0.8 mm diameter and 2 mm height.

Characterization of 3D scaffolds

FTIR assay was performed to identify functional groups in scaffolds (PPG, PP). FTIR spectra were taken in the range of wavenumbers between 4000 to 400 cm^{-1} over 20 scans at 4 cm^{-1} resolution (Bomem, model MB-102, Quebec, Canada). SEM (SEM; Philips, XL-30) examinations were used to study the surface morphology of the scaffolds (PPG, PP). The scaffolds were dried and were coated by gold sputtering (Denton Desk II Sputtering System). The surface morphology pores size and nanofiber diameter of the samples were recorded and analyzed by ImageJ software. The Contact angle measurements with water were obtained by G10 Krus's contact angle goniometer to inform about the wettability of the prepared scaffolds. For this analysis, 4 μL of the deionized water was added on the surface of the scaffolds and the contact angle was measured at 10th second under vacuum condition. TGA was performed for investigation of the thermal property of both scaffold groups under Argon atmosphere (air pressure 200) at the heating rate of 10°C/min from the temperature of 25°C to 800°C by SDT Q600 V20.9 Build 20 instrument. The mechanical properties of the scaffolds were investigated using a Universal Testing Machine (Testometric, UK). All the samples with 22 mm diameter and 10 mm height were compressed at a rate of 5 mm min^{-1} until the compression ratio reached 75%. For each group (PPG, PP), a minimum of three measurements was made and the average value was reported.

Stem cells isolation and characterization

The isolation process of hADSCs[32] was done under the support of Shahid Beheshti University's Medical Research Ethics Committee. Adipose tissue was obtained from the patients with the age of 36 ± 12 years through abdominoplasty procedures. The adipose tissues were washed using PBS, then were finely minced and digested by 1 mg/mL collagenase type I. Afterward, the cells were cultured in the growth medium of DMEM-F12 containing 10% FBS, 100 U/mL penicillin, 100 mg/mL streptomycin in an incubator at 37°C and 5% CO2. The morphology of the isolated cells was observed under a phase contrast microscope in passage 3. Then, isolated cells were characterized by cell surface markers (CD) including CD34, CD45, CD11b, CD73, CD90, and CD105 (BD Biosciences. San Jose, CA, USA) through flow cytometry technique.

Cells seeding and attachment analysis

First, the scaffolds were sterilized by dipping into ethanol 70% for 40 minutes and UV radiation for 20 minutes. After washing with PBS, 500 μL DMEM-F12 was added on each specimen and stored at 37°C in a 5% CO2 humidified atmosphere for about 24 hours. The DMEM-F12 was removed and hADSCs (3×10^6/μL) were seeded on specimens and cultured at 37°C and 5% CO2 for 21 days under growth medium (DMEM-F12,10% FBS and penicillin) for cell attachment and proliferation analysis and under osteogenic medium for cell differentiation assay. For all time point experiments, five samples of each group (PP and PPG scaffolds) in triplicate were prepared. The hADSCs seeded on tissue culture polystyrene (TCPS) were used as control.

DAPI staining was done to identify the nucleus of cells that were attached onto scaffolds. Day 1, and 14, the cell-seeded scaffolds were fixed with 4% paraformaldehyde, permeabilized with 0.1% Triton X-100, and the cell nuclei on sectioned samples were visualized using DAPI (dilution 1:2000) through an inverted fluorescent microscope (Nikon Eclipse Ti, Tokyo, Japan). SEM was performed to investigate the cells spreading morphologies on the scaffolds. For this purpose, the cell-seeded scaffolds at days 1, and 14 of culture period were washed using PBS, fixed with 2.5% glutaraldehyde (pH 7.4, 30 minutes), placed in the graded ethanol series (i.e. 30%, 50%, 70%, 90%, and 100%, respectively, each for 15 minutes). Then a thin layer of gold was put on sectioned samples and imaged by Hitachi scanning electron microscope (SEM, SU3500 Japan).

MTT assay

MTT assay was made to determine the cell viability on the scaffolds throughout the culture period at five-time points including days 1, 3, 7, 14, and 21. For this purpose, specimens were washed with PBS and incubated with MTT reagent (37°C, 4 hours) at each time point. Then, the

specimens were treated with DMSO and absorbance of formazan was evaluated with a microplate reader (BioTek EL × 800) instrument (OD = 570 nm).

Alizarin Red S staining

To confirm the synthesis of a mineralized matrix, Alizarin Red S (ARS) staining was done at days 14 and 21 of cell culture under osteogenic media. For this purpose, the cell-seeded scaffolds were fixed by 4% paraformaldehyde and stored at 4°C overnight. The specimen was washed repeatedly with PBS 3 times and was embedded in paraffin. It was sectioned and stained with 2% ARS solution for 10 minutes at room temperature. Next, the specimen was imaged by Olympus BX46 microscope. ImageJ software was used for semi-quantitative analysis of calcium deposition. In this way, five images per each group were selected randomly for each time point measurement of calcium deposition. After setting the scale, measurement items, and threshold in ImageJ software, the binary black and white images (8-bit) were obtained and analyzed. Finally, the mean of the red percentage area of images was reported on a graph.

Alkaline phosphatase activity

Alkaline phosphatase (ALP) activities were measured by the ALP assay kit (Pars Azmon, Iran) to confirm the ALP synthesis with the cell-seeded scaffolds.[33] First, 500 µL of RIPA lysis buffer was put into the cell-scaffold constructs, homogenized, and centrifuged (15 minutes at 10 000 g and 4°C), and supernatants containing total proteins were obtained. Then, 50 µL of supernatant was added to 50 µL of ALP substrate solution (p-nitrophenyl phosphate) and incubated at 37°C for 60 minutes. Next, 50 µL of NaOH (3N) was added to each well and the activity of ALP in the cell lysates was measured at 405 nm through microplate reader (BioTek EL × 800) instrument and finally the data were normalized against total proteins.

Real-time RT-PCR assays

Real-time RT-PCR assays were used to investigate the osteogenesis related genes expression including runt-related transcription factor 2 (RUNX2), collagen Iα1 (COLIα1), osteonectin (ON) and osteocalcin on cell-seeded scaffolds and TCPS under osteogenic medium at days 14 and 21. First, the total RNAs were extracted from samples with RNX-Plus™ (Cinnagen, Iran) similar to as per the manufacturer's recommendations. The ratio of absorbance at 260 nm and 280 nm was used to determine the concentration and quality of isolated RNAs. Complementary DNA (cDNA) was synthesized by 2 µg RNA based on Fermentas cDNA Synthesis Kit. Then, RT-qPCR was done in an Applied Biosystems, StepOne™ (Applied Biosystems, Bedford, MA) by using Master Mix, SYBR Green I (ABI, USA), 1 µg cDNA, ddH2O, and specific primers (Table 1). The reaction quality was confirmed by melting curve analyses. The Comparative CT Method ($2^{\Delta\Delta Ct}$) was used to determine the relative quantification of target genes and normalized to GAPDH (Reference gene) and relative to hADSCs at the fourth passage as a calibrator. Each sample was assessed at least in triplicate.

Statistical analysis

Reported data are based on mean ± standard error. The differences between groups were determined by the t test, and the P value ≤0.05 was considered to be significant.

Results

TEM analysis

The lamellar structure and the wrinkled surface of synthesized GO nanoparticles by the modified Hummer technique are clearly observed in the TEM image (Fig. 1A). Based on the image, GO nanoparticles were successfully synthesized.

FTIR analysis

In order to determine the chemical bands of polymer and nanoparticles in the scaffolds structure, FTIR spectra of the PTFE/ PVA (grey) and PTFE/PVA/GO (Blue) samples were done (Fig. 1B). The important bands related to PTFE, namely C-C chain stretch (1215 cm⁻¹), symmetric CF2 stretch (1155 cm⁻¹), CF2 wagging (639 cm⁻¹), and CF2 rocking (555 cm⁻¹) were obtained in both PVA/PTFE (PP) and PVA/PTFE/GO (PPG) scaffolds.[34,35] The bands related to PVA, namely C–OH stretching (the peak between 3300 and 3500 cm⁻¹), C-H asymmetric stretching

Table 1. Description of the primes

Genes	Primer sequence 5'-3'
h-RUNX2 Forward primer	TCT TAGAACAAATTCTGCCCTTT
h-RUNX2 Reverse primer	TGCTTTGGTCTTGAAATCACA
h-COLIα1 Forward primer	TTGTGGATGGGGACTTGTGA
h-COLIα1 Reverse primer	AGAGGCAGGTGGAGAGAGG
h-ON Forward primer	TAGAGGCTAAGTGGTGGGAGA
h-ON Reverse primer	TGAAAGGTAAAGGAGGAAATGGT
h-OC Forward primer	CCAAGGAGGGAGGTGTGTGAG
h-OC Reverse primer	AAGGGGAAGAGGAAAGAAGGGTG
h-GAPDH Forward primer	GCA GGG ATG ATG TTC TGG
h-GAPDH Reverse primer	CTT TGG TAT CGT GGA AGG AC
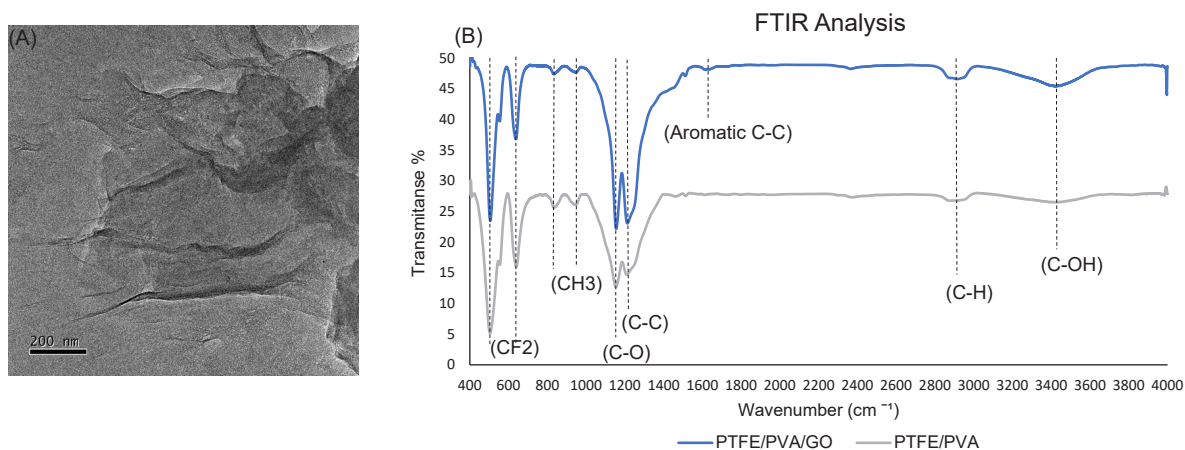
Fig. 1. The TEM analysis of synthesized GO nanoparticles (A: scale bar 200 nm). FTIR analysis of PTFE/PVA/GO (blue line) and PTFE/PVA (gray line) 3D scaffolds (B).

in CH2 and C-H symmetric stretching in CH3 (the peak between 2840 and 3000 cm^{-1}), C-O shoulder stretching (related to acetate groups), and C-C chain stretching (the two peaks between 1000 and 1400 cm^{-1}) were obtained in both scaffolds (PP, PPG).[36,37] The aromatic C-C stretching band (1624 cm^{-1}) and the intense peaks of OH and CH stretching bands were associated to GO nanoparticles in PPG scaffold.[38] Based on the FTIR report, two types of scaffolds (PP, PPG) were successfully achieved.

SEM analysis

In order to determine scaffold architecture, PP and PPG scaffolds cross-sectional thickness were prepared and observed using scanning electron microscopy (SEM) and quantified by the ImageJ software (Fig. 2). Based on the analysis, PPG scaffold (Fig. 2A-C) has multi-scale pore architecture with a diameter between 800 nm and 750 μm with 58% porosity, while the pore diameter of PP scaffold (Fig. 2D-F) is in the range of 417-750 μm, with 41% porosity. Furthermore, multiscale randomly
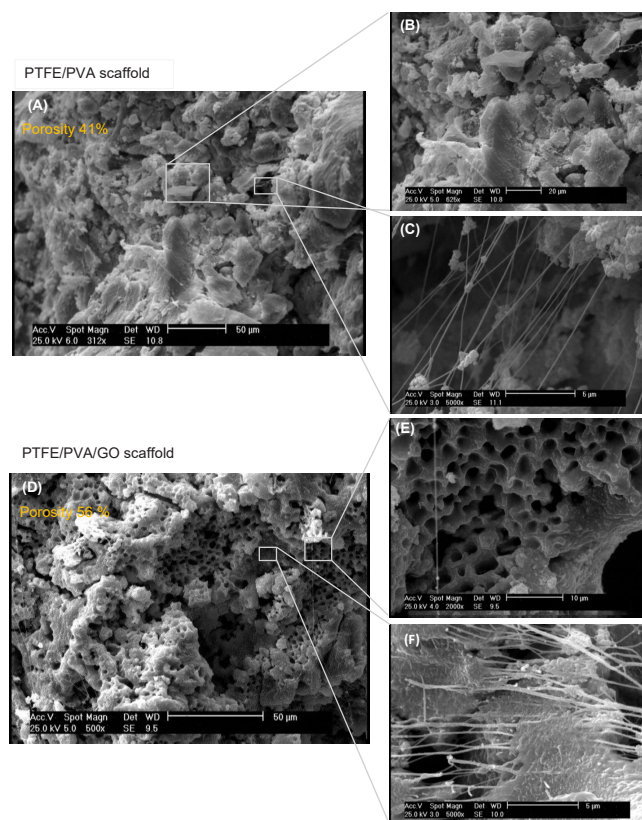
Fig. 2. SEM analysis of PTFE-PVA (A, B, C) and PTFE-PVA-GO (D, E, F) 3D scaffolds. The scale bars represent 50 μm (A, D), 20 μm (B), 10 μm (E), and 5 μm (C, F).

discontinues oriented nanofibers with a diameter between 2 and 600 nm were expanded into the 3D form of both scaffolds. Fiber density was higher in PPG scaffolds compared to those on PP scaffolds. Fiber inter-spaces were substantially enlarged in PP scaffolds compared to those on PPG scaffolds which further corroborates pore size measurements. Fiber surface morphology in PP scaffolds (smooth) and PPG scaffold (rough) are distinct.

The hydrophilic properties of PP and PPG scaffolds were defined using water contact angles (WCA) after a residence time of 10 seconds (Fig. 3). The average value of contact angle for PP scaffold was found to be 45° whereas the average value of contact angle of PPG scaffold was 15°, which clearly shows that the presence of GO nanoparticles within the PTFE/PVA matrix increased wettability of the fabricated composite scaffold type.

TGA analysis

The thermogravimetric analysis had been carried on both PTFE/PVA and PTFE/PVA/GO 3D scaffolds to study the thermal stability (Fig. 4). Thermal decomposition of both composite scaffolds (PP, PPG) showed a two-stage phenomenon (200∼400°C and 450∼600°◦C). In the first stage, temperature range from 200°C to 400°C, and the weight of PP sample (Fig. 4A) decreased gradually (10% weight loss), while PPG sample (Fig. 4B) weight declined sharply (40% weight loss). At the end of first stage, residual mass of PP (88%) and PPG (56%) were distinct. In the second degradation step, temperature range from 450°C to 600°C, both sample weight (PP, PPG) declined due to the destruction of carbon-carbon bonds in PVA, PTFE, GO components, and other residues. At the end of the second stage, the residual mass of PP sample (∼2%) was lower than that of the PPG sample (∼4%).

Compression test

Compression tests were used to investigate the mechanical performance of scaffolds (Table 2). Based on the results, both scaffolds, with and without GO nanoparticles, had similar maximum stress while the value of the break elongation (%) and extension (mm) were different which showed that GO nanoparticles affected the deformation
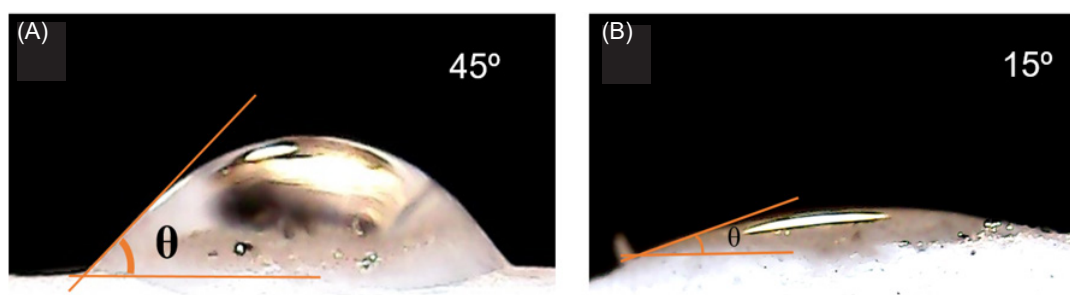
Fig. 3. Contact angle measurements of PTFE/PVA (A) and PTFE/PVA/GO (B) scaffolds.
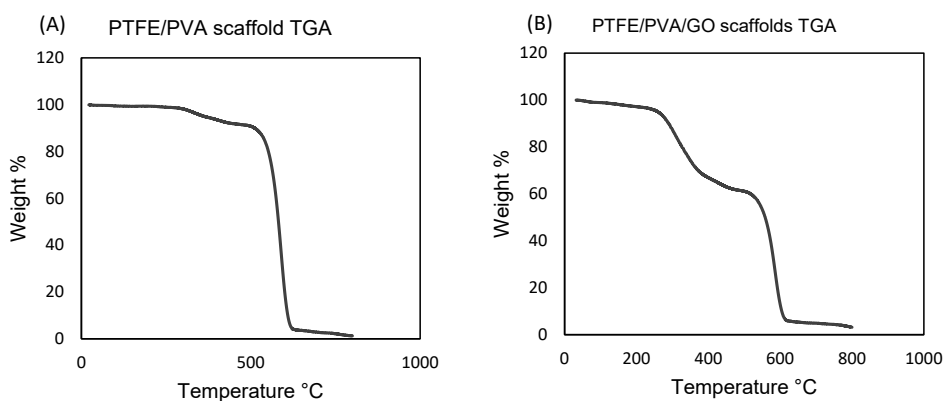
Fig. 4. Thermal analysis of PTFE-PVA (A) and PTFE-PVA-GO (B) scaffolds.

Table 2. Mechanical performance of scaffolds

Scaffold type	Maximum force (N)	Maximum extension (mm)	Maximum stress (MPa)	Maximum elongation (%)	Maximum elongation after break (%)	Module (MPa)
PTFE/PVA	-53.30	-4.05	-0.14	-40.25	8.76	0.34
PTFE / PVA /GO	-53.67	-2.12	-0.14	-21.21	-5.28	0.66

behavior of PTFE/PVA/GO scaffolds compared to PTFE/PVA composite. The Young's modulus values of 0.3 and 0.6 MPa were obtained for PTFE/PVA and PTFE/PVA/GO scaffolds, respectively. Thus, a clear trend of increasing stiffness by incorporating the GO nanoparticles was observed.

Cell isolation and characterization

The hADSCs were isolated and characterized using cell morphology through the phase-contrast microscopic image at 3rd passage and detection of mesenchymal surface marker profiles through flow cytometry. The results showed that isolated cells had typical spindle morphology of mesenchymal stem cells (Fig. 5A) and expressed CD73, CD105, and CD90, and did not exhibit any expression of CD34, CD45, and CD11b (Fig. 5B). In this way, the isolated hADSCs had mesenchymal nature.

Cells seeding characterization

The hADSCs were seeded on both scaffolds and cell attachment analysis was done by using nuclear staining (Fig. 6A-D) and SEM examinations (Fig. 6E-H) at days 1, and 14. Stained nuclei confirmed the presence of viable and adherent cells on both scaffolds. It seems that during the culture periods, the cell infiltration was occurred in both scaffolds, while cells spreading were better on PPG scaffolds compared to those on PP scaffolds.

MTT assay

The hADSCs viability on control (tissue culture polystyrene), PP, and PPG scaffolds were quantitatively examined using MTT assay at days 1, 3, 7, 14, and 21 (Fig. 7). Irrespective of the samples, the hADSCs remained viable throughout the culture period. There
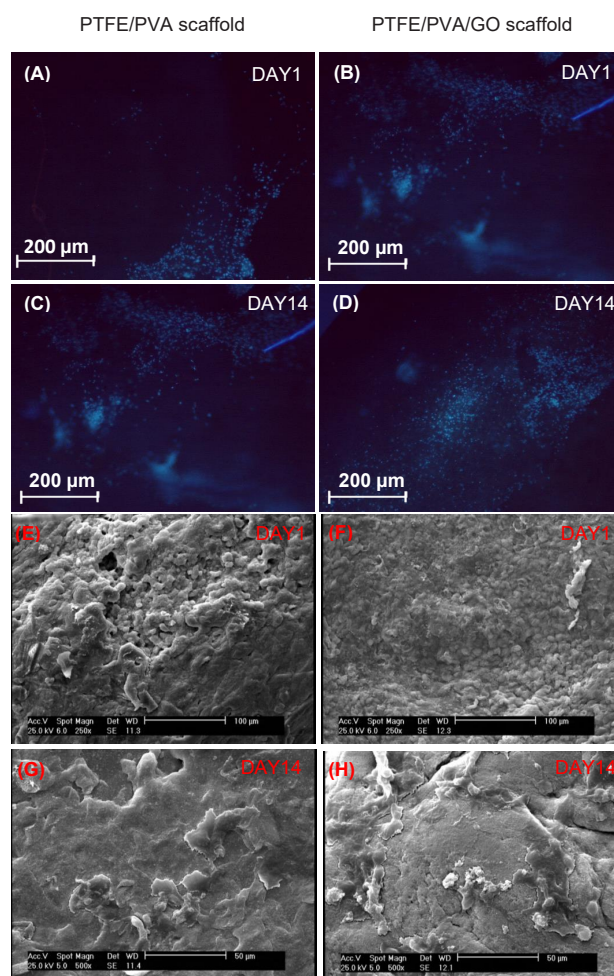
Fig. 6. Cell attachment analysis on PTFE/PVA and PTFE/PVA/GO scaffolds through DAPI staining (A, B, C, D) and SEM images (E, F, G, H) at days 1 and 14 of the culture period. Scale bar 200 μm (A-D), 100 μm (E, F), and 50 μm (G, H).
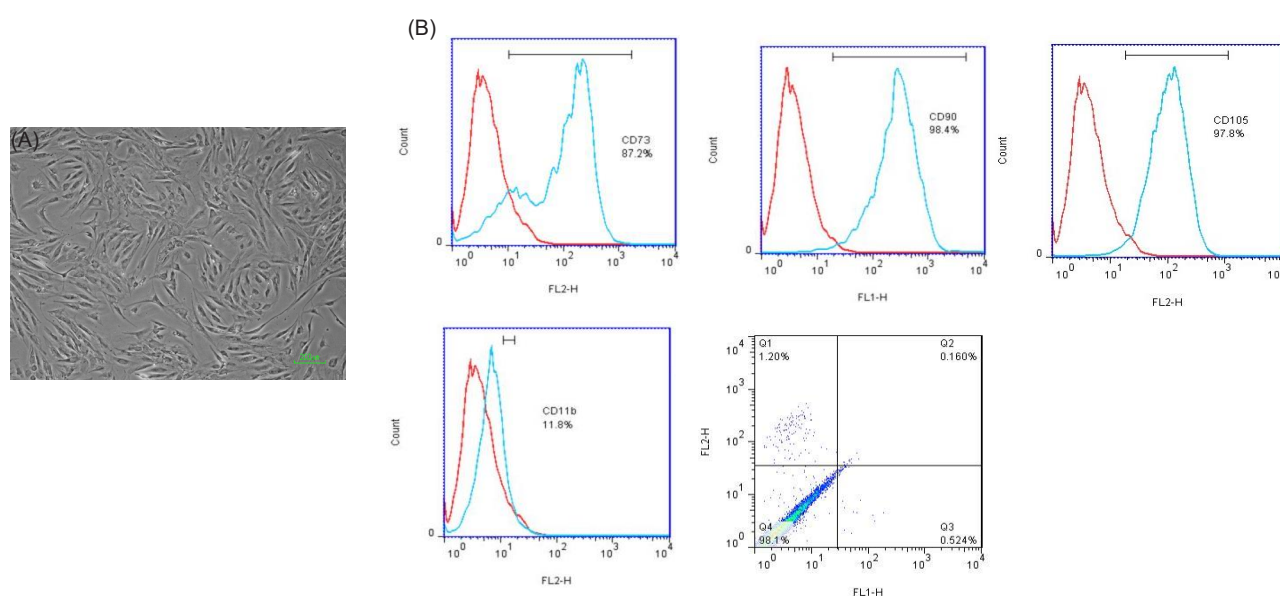
Fig. 5. Characterization of isolated hADSCs at passage three through Phase Contrast Microscopy (A: scale bar 200 μm) and Flow cytometry analysis (B).

MTT Assay
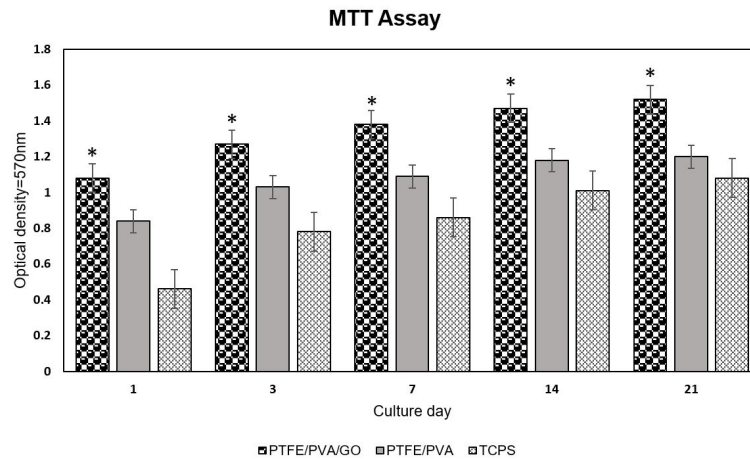
Fig. 7. Cell viability on PTFE/PVA and PTFE/PVA/GO 3D scaffolds and TCPS as a control group at days 1, 3, 7, 14, and 21 (*P*<0.05).

were statistically significant differences in the number of viable cells on PP scaffolds compared to the control at all time points of culture (*P*<0.05). There was statistically significant cell proliferation on PPG scaffolds compared to that observed on PP scaffolds and control from day 1 to day 21(*P*<0.05).

Alizarin Red S staining

In order to visualize qualitatively the calcium deposition as an osteogenic marker, samples of two scaffolds underwent the osteogenic media were stained by ARS dye at days 14 and 21 (Fig. 8A-D). As clearly observed in images, both
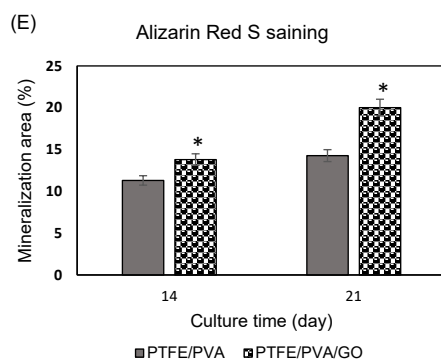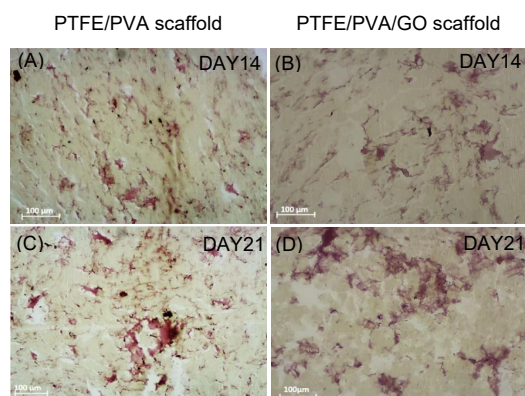
Fig. 8. Alizarin Red S staining images. Qualitative analysis (A-D), and quantitative analysis (E).

samples showed calcium deposition at two-time point measurements. As time passed, calcium deposition was increased in all samples. The percentage of the red-stained area was quantitatively higher in PPG scaffolds compared to PP scaffolds (*P*<0.05) at two-time point measurements (Fig. 8E).

ALP activity assay

In order to evaluate the osteogenic differentiation of hADSCs on control (tissue culture polystyrene), PP and PPG scaffolds underwent osteogenic media, and alkaline phosphatase (ALP) activity was determined at days 7, 14, and 21 (Fig. 9). Based on the results, all samples after 7 days in osteogenic medium showed ALP activity and as time passed, its level was increased in all samples. There were statistically significant differences in ALP activity of cells seeded on groups specimen in three-time point measurements (PPG > PP> TCPS, *P*<0.05).

Real-time PCR

To determine quantitatively differentiation of hADSCs on PP, PPG scaffolds to osteo-like cells, typical osteo-differentiation markers including Runx2, COLL Iα1, OC, and ON, were evaluated by real-time PCR at days 14 and 21 (Fig. 10).

Irrespective of the sample, the hADSCs seeded on both specimen (PP and PPG scaffolds) expressed mRNA related to Runx2, COLL Iα1, OC, and ON genes underwent osteogenic medium at two-time point measurements. The mRNA expression of Runx2 and COLL Iα1 decreased from day 14 to day 21, while OC and ON were increased during time in all samples. In corroborate with ALP activity assay, the mRNA expression of osteogenic related genes was significantly higher in PPG scaffolds specimen compared to those on PP scaffolds specimen (*P*<0.05).

Discussion

The present study aimed to fabricate and characterize 3D porous scaffolds with a new material mixture including
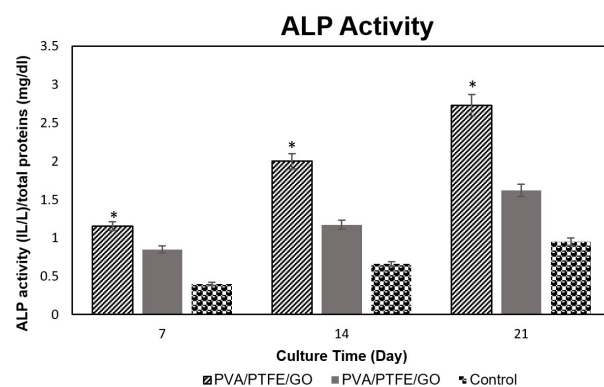
Fig. 9. ALP activity of hADSCs on PTFE/PVA and PTFE/PVA/GO 3D scaffolds and TCPS as a control group at days 7, 14, and 21 ($P<0.05$).
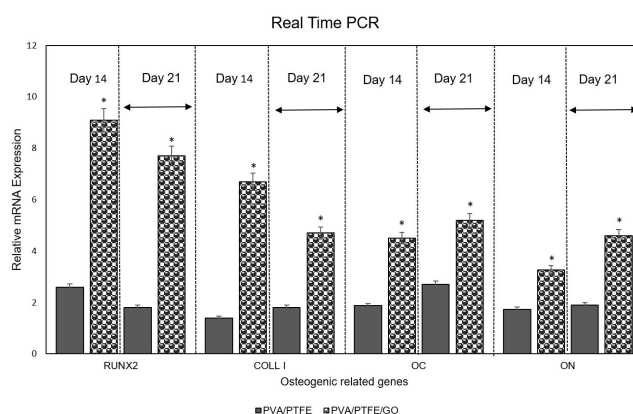
Fig. 10. Quantitative real-time PCR of the mRNA levels of RUNX2, COLL Iα, OC, and ON in hADSCs onto PTFE/PVA and PTFE/PVA/GO 3D scaffolds at days 14 and 21 of culture on osteogenic medium ($P<0.05$).

PTFE, PVA, and GO nanoparticles via freeze-drying method as a simple porous 3D scaffold fabrication method, and to investigate whether PVA with or without incorporation of GO nanoparticles improved the interaction of PTFE based scaffolds to hADSCs attachment, proliferation, and osteogenic differentiation.

For these purposes, GO nanoparticles were successfully synthesized via a modified Hummer method which has lamellar and wrinkled structural properties. Based on previous findings, the wrinkled surface provides the nanoparticles stability, good interactions with other polymers, and enhances their dispersion in the polymer composite.[39] It was demonstrated that the GO nanoparticles as a nanofiller showed high interfacial interactions with PVA matrices[40] which are a good sign that probably synthesized GO nanoparticles were dispersed on polymers mixtures.

Two types of scaffolds with and without GO nanoparticles (PP, PPG) were fabricated through chemical cross-linking with small amounts of boric acids and controlled freeze-drying method after applying high rate of stirring speed with agitating and temperature. Prior to *in vitro* cell study, the features of prepared 3D scaffolds were investigated. Based on FTIR results both scaffolds showed the important chemical bands related to the used material.

Moreover, there were not new chemical bands in FTIR results, demonstrating that the most important interaction in polymers with and without nanoparticles was probably hydrophobic and electrostatic interactions. The mechano-structural properties of biomimetic scaffolds such as pores, fibers, porosity, and stiffness affect cell behaviors like attachment, migration, spreading, proliferation, and differentiation which subsequently influence tissue ingrowth.[41] As expected, both prepared 3D scaffolds had a multiscale porous structure with a diameter between 800 nm and 750 μm in PPG scaffolds and in the range of 417-750 μm in PP scaffolds. The multiscale porous structure is necessary for new tissue ingrowth. In literature, a range of pore size for specific function including 5 μm for new functional microvascular networks, 40–100 μm for osteoid ingrowth, 100–350 μm for bone regeneration, and >500 μm for rapid vascularization are considered as optimum sizes for bone scaffolds.[1] Thus, GO incorporating scaffolds (PPG) covers all recommended pore sizes better than PP scaffolds, as well as showing higher porosity (58%) compared to PP scaffolds (41%).

Unexpected interesting findings in scaffold surface morphology analysis were the existence of randomly oriented nanofibers in range 2 and 650 nm in both scaffolds which are comparable to nanofibers produced

by electrospinning as a widely used nanofibers fabrication methods.[42] The random nano-sized fibers in 3D scaffolds could simulate the natural ECM of bone tissue and subsequently improve the organization of actin cytoskeleton, integrin-mediated adhesion points, and also modulation of osteogenic differentiation.[43] Previous reports showed that stem cell migration on nanofibers between 200 and 700 nm was better than those on microfiber (1.4–4 μm), as well as hMSCs giving rise to osteogenic cell lineage (<400 nm) faster than those occurred on microfibers (1.1–5.7 μm).[44] Thus, according to the above-mentioned evidence, the existence of fibers in both fabricated scaffolds (PP, PPG) endowed nano-sized topographical features to structure and could be desirable for BTE. Notably, the differences in both scaffolds architecture were ascribed to the incorporation of GO nanoparticles in PPG scaffolds which reduce the diameter of pore and fiber and also convert smoothly to irregular surface fiber.[36]

To the best of our knowledge, this study is the first report of the micro/nanoporous and nanofibrous 3D structure fabrication in a one-step freeze-drying approach that provides nanotopographical cures for cell behaviors. It could be the result of selected materials, their interactions (PTFE, PVA, and GO nanoparticle) and/or controlled parameters in the freeze-drying method and fabrication process. There are several reports on the fabrication of these architectures in a single 3D scaffold with freeze-drying and other methods such as electrospinning[45] and thermally induced self-agglomeration (TISA)[46] through the multistep approach. Our results showed a freeze-drying method not as a process for the fabrication of 3D structures, but as a new way to produce a nanofibrous environment.

The behavior of the scaffolds in the presence of water is a critical item that will affect the success of tissue engineering substitute. According to the contact angle measurements, both scaffolds were considered as hydrophilic surface templates which could support the cells adhesion and proliferation .[47] These findings, θ value for PPG (15°) and PP (45°) scaffolds, corroborated our FTIR and surface structural analysis results and also previous findings which showed the higher concentration of GO nanoparticles in scaffold structure may result in the elevation of wettability degree due to the high density of OH groups on the composite scaffold surface.[48]

TGA results, in support of previous findings, showed that the presence of GO and PTFE nanoparticles improves the thermal resistance of PVA nanocomposites to degradation at higher temperatures (>350 °C).[49,50] Previous reports showed that PTFE reinforced by graphene nanoplate as a filler had the same melting temperature (Tm) to that of pure PTFE (Tm=317°C) but the degree of crystallinity (X_c) was significantly increased.[51] According to our results, improvement of thermal stability of PTFE/PVA with the addition of GO nanoparticles was not significant. It could

be explained by increasing the –O containing groups in composite after incorporation of GO nanoparticles, and also probably the mobility behavior of carbon-carbon polymer skeleton.[51,52]

The deformation behavior of the scaffolds was examined using compression tests. PP and PPG scaffolds revealed respective compressive modulus of 130 and 620 kPa which means that the PPG scaffold is stiffer than PP scaffold. Like previous findings, the modulus increment in PPG scaffolds is attributed to the reinforcing function of GO nanoparticles.[53] It was demonstrated that GO nanoparticles as a green nanofiller improved the mechanical strength and thermal stability of different composites in a dose-dependent manner.[54] According to previous evidence, the addition of 0.8 wt% of GO nanoparticles to neat PVA hydrogel improved the tensile strength and compressive strength to 132% and 36%.[55] Moreover, incorporation of GO nanoparticles in PTFE/glass fabric (GF) composite improved the tensile strength and toughness to 25.1 MPa and 20.2 MJ/m3.[56] Notably, scaffolds stiffness play an important role in cell behaviors including adhesion, spreading, migration, and differentiation. In literature, cells migrate toward the higher stiff substitute and spread strongly.[57] It was demonstrated that bone marrow mesenchymal stem cells give rise to osteogenic phenotype when cultured on a substitute with 25-40 KPa stiffness which is similar to pre-mineralized bone.[58]

For the investigation of cell behaviors on the scaffolds, hADSCs were successfully isolated and characterized and were seeded on both scaffolds. As evidenced by Fig. 6, the cells tended to be in contact with one another and interaction, especially on PPG scaffolds. This could be explained by the high porosity, stiffness and protein adsorption due to the incorporation of GO nanoparticles in PPG scaffolds which provide a well microenvironment for cell adhesion and spreading.[59] Furthermore, cell proliferation occurred on both scaffolds during culture time, but the cells on PPG scaffolds significantly were higher than those on PP scaffolds and controls. This occurrence may be assigned to the highly hydrophilic nature of PPG scaffolds (WCA=15°) and highly porous

and fibrous structures due to the incorporation of GO nanoparticles. It was shown that GO-applied scaffold has a toxic effect on cell viability in a dose-dependent manner.[60] This study like previous findings showed GO nanoparticles in the safe dose (≤0.1 µg/mL)[61] had no toxic effect on cell proliferation but rather improved it. Furthermore, several investigators have presented similar results indicating that low dose of GO nanoparticles has positive bio-effects on the cellular activities and fate owing to a combination of factors including nanostructured surfaces, surface topography, strong stiffness, high surface energy, reactive oxygen functional groups, and adsorption of proteins.[62,63] Moreover, there are statistical differences in cell proliferation between PP scaffolds and control. This occurrence may be ascribed to moderately hydrophilic nature (θ=45°), as well as the suitable pore and fiber 3D structure in PP scaffolds which present topographical features for cells.

Osteogenic differentiation of hADSCs on PP and PPG scaffolds underwent osteogenic media were studied by visualizing the calcium deposition through ARS staining, determining the amount of ALP activity, and also the mRNA expression of typical osteo-differentiation markers including Runx2 and COLL Iα as early osteogenic markers, and OC and ON as late osteogenic markers.

There are significant statistical differences in ALP activity, calcium deposition and osteogenic related genes expression in PTFE/PVA/GO seeded scaffolds as compared to PTFE/PVA seeded scaffolds in all time point measurements. Furthermore, the levels of osteogenic related markers in PTFE/PVA seeded scaffolds were higher than those on TCPS. These results could be explained by the following reasons: both scaffolds had 3D structures and provided better milieu for cell behaviors as compared to 2D culture; moreover, both scaffolds had nano topographical features. Previous evidence showed that nanopattern (650 nm) increased differentiation towards osteogenic lineages underwent specific differentiation media.[64] Additionally, GO incorporated scaffolds had the capability for the absorption of osteogenic differentiation factors in medium and enhanced the differentiation process.[30]

Conclusion

This is the first study that prepared multiscale pores and nanofibrous 3D scaffolds by using the ternary composition of PTFE, PVA, and GO nanoparticles using cross-linker and freeze-drying process. As expected, PVA improved the wettability of PTFE polymer and also GO nanoparticles improved scaffold stiffness and wettability. Both scaffolds had a nano-topographical structure which supported cell attachment, proliferation, and differentiation. The GO incorporated scaffold (PPG) showed better multiscale pore sizes, fewer fiber diameters, higher porosity, good stiffness and appropriate cell attachment, proliferation, and osteogenic differentiation. An interesting result in

this study was the production of nanofibers in the range 2 to 650 nm using one step freeze-drying methods that are comparable with electrospun nanofiber diameter. In addition, PTFE polymer as a hydrophobic polymer in the composite successfully blended homogeneously with PVA and GO nanoparticles and had an effective role in the improvement of mechanical and thermal stability of scaffolds and also had no toxic effect on cell proliferation. Based on this study, PTFE/PVA and PTFE/PVA/GO scaffolds could be employed for BTE approaches.

Ethical statement
This study is under the support of Shahid Beheshti University's Medical Research Ethics Committee (IR.SBMU.REC.1398.026).

Competing interests
There are no competing interests to declare.

Authors' contribution
All authors equally contributed to this study.

References
1. Henkel J, Woodruff MA, Epari DR, Steck R, Glatt V, Dickinson IC, et al. Bone regeneration based on tissue engineering conceptions—a 21st century perspective. *Bone Res* **2013**;1:216-248. doi:10.4248/BR201303002
2. Kashirina A, Yao Y, Liu Y, Leng J. Biopolymers as bone substitutes: a review. *Biomater Sci* **2019**;7:3961-83. doi:10.1039/C9BM00664H.
3. Jenkins TL, Little D. Synthetic scaffolds for musculoskeletal tissue engineering: cellular responses to fiber parameters. *NPJ Regen Med* **2019**;4:15. doi:10.1038/s41536-019-0076-5
4. Caddeo S, Boffito M, Sartori S. Tissue engineering approaches in the design of healthy and pathological in vitro tissue models. *Front Bioeng Biotech* **2017**;5:40. doi:10.3389/fbioe.2017.00040
5. Prince E, Kumacheva E. Design and applications of man-made biomimetic fibrillar hydrogels. *Nat Rev Mater* **2019**;4:99-115. doi:10.1038/s41578-018-0077-9
6. Amruthwar SS, Janorkar AV. In vitro evaluation of elastin-like polypeptide–collagen composite scaffold for bone tissue engineering. *Dent Mater J* **2013**;29:211-220. doi:10.1016/j.dental.2012.10.003.
7. Nudelman F, Pieterse K, George A, Bomans PH, Friedrich H, Brylka LJ et al. The role of collagen in bone apatite formation in the presence of hydroxyapatite nucleation inhibitors. *Nat Mater* **2010**;9:1004. doi:10.1038/nmat2875
8. Kalka M, Zoglowek A, Ożyhar A, Dobryszycki P. Proteins in Calcium Phosphate Biomineralization. *IntechOpen* **2019**. doi:10.5772/intechopen.86718
9. Wang X, Kim HJ, Wong C, Vepari C, Matsumoto A, Kaplan DL. Fibrous proteins and tissue engineering. *Mater Today* **2006**;9:44-53. doi:10.1016/S1369-7021(06)71742-4.
10. Greenland KN, Carvajal MFCA, Preston JM, Ekblad S, Dean WL, Chiang JY, et al. Order, Disorder, and Temperature-Driven Compaction in a Designed Elastin Protein. *J Phys Chem B* **2018**;122: 2725-2736.doi:10.1021/acs.jpcb.7b11596
11. Singla A, Lee CH. Effect of elastin on the calcification rate of

collagen-elastin matrix systems. *J Biomed Mater Res* **2002**;60:368-374. doi:10.1002/jbm.10077

12. Wang J-Z, You M-L, Ding Z-Q, Ye W-B. A review of emerging bone tissue engineering via PEG conjugated biodegradable amphiphilic copolymers. *Mater Sci Eng C Mater Biol Appl* **2019**;97:1021-1035. doi: 10.1016/j.msec.2019.01.057

13. Jiang H, Duan L, Ren X, Gao G. Hydrophobic association hydrogels with excellent mechanical and self-healing properties. *Eur Polym J* **2019**;112:660-669. doi:10.1016/j.eurpolymj.2018.10.031

14. Baht GS, Hunter GK, Goldberg HA. Bone sialoprotein–collagen interaction promotes hydroxyapatite nucleation. *Matrix Biol* 2008;27:600-608. doi:10.1016/j.matbio.2008.06.004

15. Kyriakides TR. Molecular Events at Tissue–Biomaterial Interface. *Host Response to Biomaterials*. Elsevier; **2015**. p. 81-116. doi:10.1016/B978-0-12-800196-7.00005-0

16. Zanchetta P, Guezennec J. Surface thermodynamics of osteoblasts: relation between hydrophobicity and bone active biomaterials. *Colloids Surf B Biointerfaces* **2001**;22:301-307. doi:10.1016/S0927-7765(01)00200-4.

17. Phadke A, Zhang C, Hwang Y, Vecchio K, Varghese S. Templated mineralization of synthetic hydrogels for bone-like composite materials: Role of matrix hydrophobicity. *Biomacromolecules* **2010**;11:2060-2068. doi:10.1021/bm100425p

18. Jansen EJ, Sladek RE, Bahar H, Yaffe A, Gijbels MJ, Kuijer R, et al. Hydrophobicity as a design criterion for polymer scaffolds in bone tissue engineering. *Biomaterials* **2005**;26:4423-4431.doi:10.1016/j.biomaterials.2004.11.011

19. Gabriel M, Niederer K, Frey H. Wet chemistry and peptide immobilization on polytetrafluoroethylene for improved cell-adhesion. *J Vis Exp* **2016**(114):e54272. doi:10.3791/54272

20. Gabriel M, Niederer K, Becker M, Raynaud CM, Vahl C-F, et al. Tailoring Novel PTFE Surface Properties: Promoting Cell Adhesion and Antifouling Properties via a Wet Chemical Approach. *Bioconjug Chem* **2016**;27:1216-1221. doi:10.1021/acs.bioconjchem.6b00047

21. Wise SG, Waterhouse A, Kondyurin A, Bilek MM, Weiss AS. Plasma-based biofunctionalization of vascular implants. *Nanomedicine (Lond)* **2012**;7:1907-1916. doi:10.2217/nnm.12.161.

22. Mikulikova R, Moritz S, Gumpenberger T, Olbrich M, Romanin C, Bacakova L, et al. Cell microarrays on photochemically modified polytetrafluoroethylene. *Biomaterials* **2005**;26:5572-80. doi:10.1016/j.biomaterials.2005.02.010

23. Serrano-Aroca Á. Enhancement of Hydrogels' Properties for Biomedical Applications: Latest Achievements. *Hydrogels* **2018**:91. doi:10.5772/intechopen.71671

24. Li M, Chen F, Liu C, Qian J, Wu Z, Chen Z. Electrospun Fibrous PTFE Supported ZnO for Oil–Water Separation. *J Inorg Organomet Polym Mater* **2019**:1-8. doi:10.1007/s10904-019-01135-x

25. Kim H, Lee Y, Kim Y, Hwang Y, Hwang N. Biomimetically reinforced polyvinyl alcohol-based hybrid scaffolds for cartilage tissue engineering. *Polymers (Basel)* **2017**;9:655.doi:10.3390/polym9120655

26. Kumar A, Han SS. PVA-based hydrogels for tissue engineering: a review. *INT J POLYM MATER* **2017**;66:159-182.doi:10.1080/00914037.2016.1190930

27. Shuai C, Feng P, Gao C, Shuai X, Xiao T, Peng S. Graphene oxide reinforced poly (vinyl alcohol): nanocomposite scaffolds for tissue engineering applications. *RSC Adv* **2015**;5:25416-25423. doi:10.1039/C4RA16702C

28. Eivazzadeh-Keihan R, Maleki A, de la Guardia M, Bani MS, Chenab KK, Pashazadeh-Panahi P, et al. Carbon based nanomaterials for tissue engineering of bone: Building new bone on small black scaffolds: A review. *J Adv Res* **2019**; 18:185-201. doi:10.1016/j.jare.2019.03.011

29. Prasadh S, Suresh S, Wong R. Osteogenic potential of graphene in bone tissue engineering scaffolds. *Materials (Basel)* **2018**;11:1430. doi:10.3390/ma11081430

30. Li M, Xiong P, Yan F, Li S, Ren C, Yin Z, et al. An overview of graphene-based hydroxyapatite composites for orthopedic applications. *Bioact Mater* **2018**;3:1-18. doi:10.1016/j.bioactmat.2018.01.001

31. Mahmoudifard M, Soleimani M, Hatamie S, Zamanlui S, Ranjbarvan P, Vossoughi M, et al. The different fate of satellite cells on conductive composite electrospun nanofibers with graphene and graphene oxide nanosheets. *Biomed Mater* **2016**;11:025006. doi:10.1088/1748-6041/11/2/025006

32. Zuk PA, Zhu M, Ashjian P, De Ugarte DA, Huang JI, Mizuno H, et al. Human adipose tissue is a source of multipotent stem cells. *Mol Biol Cell* 2002;13:4279-4295. doi:10.1091/mbc.e02-02-0105

33. Izadpanahi M, Seyedjafari E, Arefian E, Hamta A, Hosseinzadeh S, Kehtari M, et al. Nanotopographical cues of electrospun PLLA efficiently modulate non-coding RNA network to osteogenic differentiation of mesenchymal stem cells during BMP signaling pathway. *Mater Sci Eng C Mater Biol Appl* **2018**;93:686-703. doi:10.1016/j.msec.2018.08.023

34. Gill FS, Chandra S, Panwar V, Uniyal D, Kalra G, Kumar V, et al. Conduction pathways in CNF/PTFE composite: air oxidized CNFs coated with the incomplete layer of PTFE. *Diam Relat Mater* **2018**;89:227-238. doi:10.1016/j.diamond.2018.08.015

35. Hannon M, Boerio F, Koenig J. Vibrational analysis of polytetrafluoroethylene. *J Chem Phys* **1969**;50:2829-2836. doi:10.1063/1.1671471

36. Wang S, Zhang Z, Chen B, Shao J, Guo Z. Self-healing hydrogel of poly (vinyl alcohol)/graphite oxide with p H-sensitive and enhanced thermal properties. *J Appl Polym Sci* **2018**;135:46143. doi:10.1002/app.46143

37. Yang H, Xu S, Jiang L, Dan Y. Thermal decomposition behavior of poly (vinyl alcohol) with different hydroxyl content. *J MACROMOL SCI B* **2012**;51:464-480. doi:10.1080/00222348.2011.597687.

38. Yu H, Zhang B, Bulin C, Li R, Xing R. High-efficient synthesis of graphene oxide based on improved hummers method. *Sci Rep* **2016**;6:36143. doi:10.1038/srep36143.

39. Deng S, Berry V. Wrinkled, rippled and crumpled graphene: an overview of formation mechanism, electronic properties, and applications. *Mater Today* **2016**;19:197-212. doi:10.1016/j.mattod.2015.10.002.

40. Li Y, Umer R, Samad YA, Zheng L, Liao K. The effect of the ultrasonication pre-treatment of graphene oxide (GO) on the mechanical properties of GO/polyvinyl alcohol composites. *Carbon* 2013;55:321-327. doi:10.1016/j.carbon.2012.12.071.

41. Chen X, Fan H, Deng X, Wu L, Yi T, Gu L, et al. Scaffold structural microenvironmental cues to guide tissue regeneration in bone tissue applications. *Nanomaterials (Basel)* **2018**;8:960. doi:10.3390/nano8110960.

42. Bhattarai DP, Aguilar LE, Park CH, Kim CS. A review on properties of natural and synthetic based electrospun fibrous materials for bone tissue engineering. *Membranes (Basel)* **2018**;8:62. doi:10.3390/membranes8030062.

43. Wang B, Cai Q, Zhang S, Yang X, Deng X. The effect of poly (L-lactic acid) nanofiber orientation on osteogenic responses of human osteoblast-like MG63 cells. *J Mech Behav Biomed Mater* **2011**;4:600-609. doi:10.1016/j.jmbbm.2011.01.008.

44. Jenkins TL, Little D. Synthetic scaffolds for musculoskeletal tissue engineering: cellular responses to fiber parameters. *NPJ Regen Med* **2019**;4:1-14. doi:10.1038/s41536-019-0076-5.

45. Uzunalan G, Ozturk MT, Dincer S, Tuzlakoglu K. A newly designed collagen-based bilayered scaffold for skin tissue regeneration. *J Compos Biodegrad Polym* **2013**;1:8-15. doi:10.12974/2311-8717.2013.01.01.2.

46. Xu T, Miszuk JM, Zhao Y, Sun H, Fong H. Electrospun polycaprolactone 3D nanofibrous scaffold with interconnected and hierarchically structured pores for bone tissue engineering. *Adv Healthc Mater* **2015**;4:2238-2246. doi:10.1002/adhm.201500345.

47. Chang H-I, Wang Y. Cell responses to surface and architecture of tissue engineering scaffolds. Regenerative medicine and tissue engineering-cells and biomaterials. *InTechOpen* **2011**. doi:10.5772/21983

48. Deshmukh K, Khatake S, Joshi GM. Surface properties of graphene

oxide reinforced polyvinyl chloride nanocomposites. *J Polym Res* **2013**;20:286. doi:10.1007/s10965-013-0286-2

49. Avella M, Errico M, Rimedio R. PVA/PTFE nanocomposites: Thermal, mechanical, and barrier properties. *J Mater Sci* **2004**;39:6133-6136. doi:10.1023/B:JMSC.0000041718.18548.10

50. Kim S, Shimazu J, Fukaminato T, Ogata T, Kurihara S. Thermal conductivity of graphene oxide-enhanced polyvinyl alcohol composites depending on molecular interaction. *Polymer* **2017**;129:201-206.doi:10.1016/j.polymer.2017.09.055

51. Cai X, Jiang Z, Zhang X, Gao T, Yue K, Zhang X. Thermal property improvement of polytetrafluoroethylene nanocomposites with graphene nanoplatelets. *RSC Adv* **2018**;8:11367-11374. doi:10.1039/C8RA01047A

52. Sengupta I, Chakraborty S, Talukdar M, Pal SK, Chakraborty S. Thermal reduction of graphene oxide: How temperature influences purity. *J Mater Sci* **2018**;33:4113-4122. DOI:10.1557/jmr.2018.338

53. Sharma S, Prakash J, Pujari P. Effects of the molecular level dispersion of graphene oxide on the free volume characteristics of poly (vinyl alcohol) and its impact on the thermal and mechanical properties of their nanocomposites. *Phys Chem Chem Phys* **2015**;17:29201-29209. doi:10.1039/C5CP05278E

54. Yang S, Liu Y, Jiang Z, Gu J, Zhang D. Thermal and mechanical performance of electrospun chitosan/poly (vinyl alcohol) nanofibers with graphene oxide. *Adv Compos Hybrid Mater* **2018**;1:722-730. doi:10.1007/s42114-018-0060-3

55. Zhang L, Wang Z, Xu C, Li Y, Gao J, Wang W, et al. High strength graphene oxide/polyvinyl alcohol composite hydrogels. *J Mater Chem* **2011**;21:10399-10406. doi:10.1039/C0JM04043F

56. Zhang B, Han J. Strong nanocomposites reinforcement effects in PTFE/glass fabric composites modified with graphene. *Compos Interfaces* **2019**;26:525-535. doi:10.1080/09276440.2018.1511216

57. Bangasser BL, Shamsan GA, Chan CE, Opoku KN, Tüzel E, Schlichtmann BW, et al. Shifting the optimal stiffness for cell migration. *Nat Commun* **2017**;8:15313. doi:10.1038/ncomms15313

58. Sun M, Chi G, Li P, Lv S, Xu J, Xu Z, et al. Effects of matrix stiffness on the morphology, adhesion, proliferation and osteogenic differentiation of mesenchymal stem cells. *Int J Med Sci* **2018**;15:257. doi:10.7150/ijms.21620

59. Halim A, Luo Q, Ju Y, Song G. A mini review focused on the recent applications of graphene oxide in stem cell growth and differentiation. *Nanomaterials (Basel)* **2018**;8:736. doi:10.3390/nano8090736

60. Nishida E, Miyaji H, Kato A, Takita H, Iwanaga T, Momose T, et al. Graphene oxide scaffold accelerates cellular proliferative response and alveolar bone healing of tooth extraction socket. *Int J Nanomedicine* **2016**;11:2265. doi:10.2147/IJN.S104778

61. Wei C, Liu Z, Jiang F, Zeng B, Huang M, Yu D. Cellular behaviours of bone marrow-derived mesenchymal stem cells towards pristine graphene oxide nanosheets. *Cell Prolif* **2017**;50:e12367. doi:10.1111/cpr.12367

62. Zhang Y, Wu C, Guo S, Zhang J. Interactions of graphene and graphene oxide with proteins and peptides. *Nanotechnol Rev* **2013**;2:27-45. doi:10.1515/ntrev-2012-0078

63. Lee WC, Lim CHY, Shi H, Tang LA, Wang Y, Lim CT, et al. Origin of enhanced stem cell growth and differentiation on graphene and graphene oxide. *ACS Nano* **2011**;5:7334-7341. doi:10.1021/nn202190c

64. Abagnale G, Steger M, Nguyen VH, Hersch N, Sechi A, Joussen S, et al. Surface topography enhances differentiation of mesenchymal stem cells towards osteogenic and adipogenic lineages. *Biomaterials* **2015**;61:316-326. doi:10.1016/j.biomaterials.2015.05.030